IEEE Instrumentation and Measurement
Technology Conference
Baltimore, MD, USA, May 1-4, 2000

# Object Recognition Using Pseudo-random Color Encoded Structured Light

E.M. Petriu [(1)], Z. Sakr[(1)] , H.J.W. Spoelder [(2)], and A. Moica [(1)]

[(1)]School of Information Technology and Engineering, University of Ottawa, Canada,
[(2)] Department of Computer Science, The Free University of Amsterdam, The Netherlands

## Abstract

*This paper discusses a new structured light technique using multi-valued pseudo-random color encoded grid patterns. This encoding completely solves the point identification problem allowing for an absolute identification of both the line- and column-index of any individual grid node projected on a surface. The use of multi-valued sequences instead of binary sequences has the notable advantage of a more compact encoding which eventually leads to higher measurement precision.*

## 1. Introduction

Structured light is an efficient technique for obtaining 3D scene information from a single 2D image by using a specially designed light source to project sheets or beams of light with a known *a priori* spatial distribution onto the scene casting lines or points (dots) on objects [1]-[4].

Object surfaces are supposed to be Lambertian so the incident light is scattered by the surface and the perceived brightness is independent of the direction of view, [5]. A camera is used to visualize, from an angle, the structured light projection on the surface. Recovery of the 3D coordinates of different points identified on an object's surface is based on the triangulation principle [6].

There are different patterns that can be used for structured light applications: (i) single point, (ii) single line (iii) stripe pattern, and (iv) grid pattern.

The grid pattern combines the advantages of both the simple point and the line pattern as sharp discontinuities may indicate jump boundaries at several object points. Grid coding imposes only weak constraints on the physical objects which are measured, [7]:

(i) Object surfaces are "smooth" in the sense that the spatial frequency of surface undulations is smaller than the grid's spatial frequency. This allows the capture of essential features of the object's surface, as there are only small changes in the surface geometry between consecutive grid lines.

(ii) Surfaces are "much" larger than grid spacing so that multiple grid nodes cover any surface.

All information produced by a grid pattern can be captured from a single snapshot of the illuminated object surface which has the advantage of accelerating the ranging process. The simultaneous generation of all grid nodes and/or lines may introduce ambiguity in the identification of individual nodes or lines projected on object surfaces resulting in the so called *point identification problem* similar to the *correspondence problem* encountered in stereo vision.

This paper discusses a new structured light technique using a pseudo-random multi-valued color encoded grid pattern. This encoding completely solves the point identification problem as it allows for an absolute identification of both grid coordinates, the line- and column-index, of any grid node projected on an object's surface, Fig. 1.

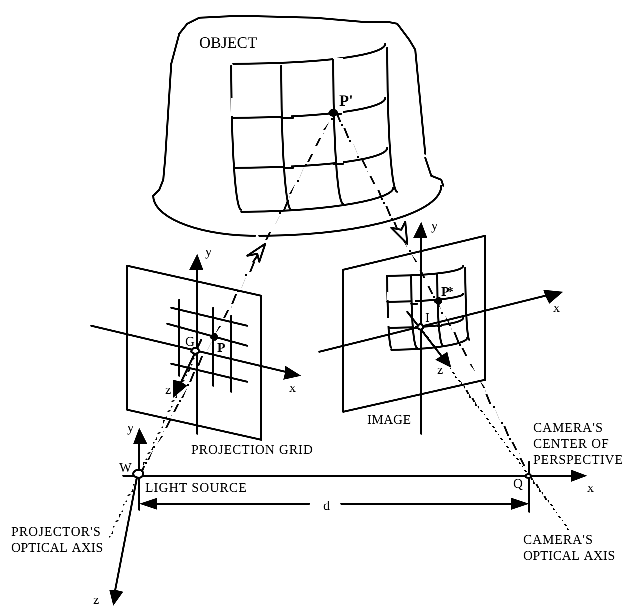


Fig. 1. Point identification in grid encoded structured light.

## 2. Grid indexing using pseudo-random multi-valued encoding

The projection grid has the row- and column-lines color encoded with the terms of two *pseudo-random multi-valued sequences* (PRMVS). Such a sequence has multi-valued elements taken from an alphabet of $q$ symbols, where $q$ is a prime or a power of a prime. A $(q^n - 1)$ -term PRMVS is generated by an $n$-position shift register with a feedback path specified by a primitive polynomial $h(x) = x^n + h_{n-1} \cdot x^{n-1} + ... + h_1 \cdot x + h_0$ of degree $n$ with coefficients from the Galois field $GF(q)$, [8]. When $q$ is a power of a prime, $q = p^m$, the Galois field elements are expressed as the first $q-1$ powers of some primitive element, labeled here by the letter $A$: $GF(q) = \{0,1,A,A^2,...,A^{q-2}\}$.

Primitive polynomials over $GF(q) = \{0,1,A,A^2,...,A^{q-2}\}$

| n | q=3 | q=4 | q=8 |
|---|---|---|---|
| 2 | $x^2+x+2$ | $x^2+x+A$ | $x^2+Ax+A$ |
| 3 | $x^3+2x+1$ | $x^3+x^2+x+A$ | $x^3+x+A$ |
| 4 | $x^4+x+2$ | $x^4+x^2+Ax+A^2$ | $x^4+x+A^3$ |
| 5 | $x^5+2x+1$ | $x^5+x+A$ | $x^5+x^2+x+A^3$ |
| 6 | $x^6+x+2$ | $x^6+x^2+x+A$ | $x^6+x+A$ |

According to the PRMVS *window property* any $q$-valued contents observed through an *n-position* window sliding over the PRMVS is unique and fully identifies the current position of the window.

A translation from the pseudo-random binary code into the more convenient natural binary representation is always necessary for practical applications. A strictly parallel solution would be to use a look-up code conversion table. This is expensive equipment-wise for applications that require high-resolution measurements. At the other extreme, a strictly serial translation exploits the reversibility of the PRMVS generating algorithm. This method is based on the idea that it is possible to find the natural value associated with any pseudo-random code by simply counting the number of reverse feedback shifts that it takes for the given pseudo-random code to arrive back into the "zero position" pattern. This solution takes a relatively long time for high-resolution measurements.

A compromise solution combines features of both serial and parallel methods [9]. Certain positions of the PRS, uniformly distributed with a period of $t$, are employed as "milestones". Let it be a position $p = m \cdot t + r$, where $m \cdot t$ is the position of the nearest "down the track milestone" $Q(m)$ and $r$ represents the position relative to this milestone. The natural code for $r$ is found by counting the steps required to arrive by successive back shifts from the initial code to the nearest milestone $Q(m)$. All intermediate states of this serial shift-back operation are checked in parallel against all possible "milestone" pseudo-random patterns. The code conversion of the relative position $r$ distance is found serially while the "milestone" code conversion is done in parallel.

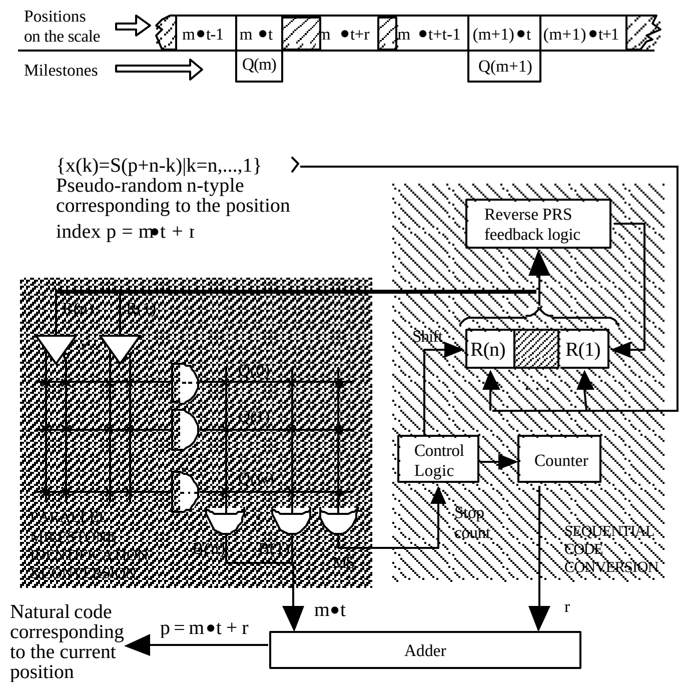


Fig. 2. Serial-parallel pseudo-random/natural decoder.

In our experiment we used a grid, as illustrated in Fig. 3, with row- and column-lines are each color encoded with the terms of a 15-term PRMVS: $\{0, 1, 1, A^2, 1, 0, A, A, 1, A, 0, A^2, A^2, A, A^2\}$. This sequence is generated by a two stage shift register, n=2, having the feedback path defined by the primitive polynomial $h(x) = x^2+x+A$ over $GF(4) = \{0,1,A,A^2\}$, with $A^2+A+1=0$ and $A^3=1$. Any 2-tuple seen through a window sliding over this sequence is unique.

The row-index $i$ of a given grid node (i,j) can be recovered by identifying the X(i) and X(i+1) [or X(i-1)] associated with two adjacent row lines. The column-index $j$ can be recovered by identifying the Y(j) and Y(j+1) [or Y(j-1)] associated with two adjacent column lines.

The choice of the encoding colors could be essential in real life applications being influenced by the ambient lighting and by the particular color of the objects. In order to find the best compromise for a given situation, we are using an original *opportunistic-adaptive color assignment* technique. Using a computer projector, we are able to change in real-time (supposing that the object is stationary during the length of the experiment) the colors of the structured light lines. A series of mono-colored grids are projected on the scene and the colors that give the sharpest definition of the projected grid in the recovered images are retained. The best colors are then assigned to marking the *q* distinct values (in this specific case *q*=4) of the PRMVS elements.

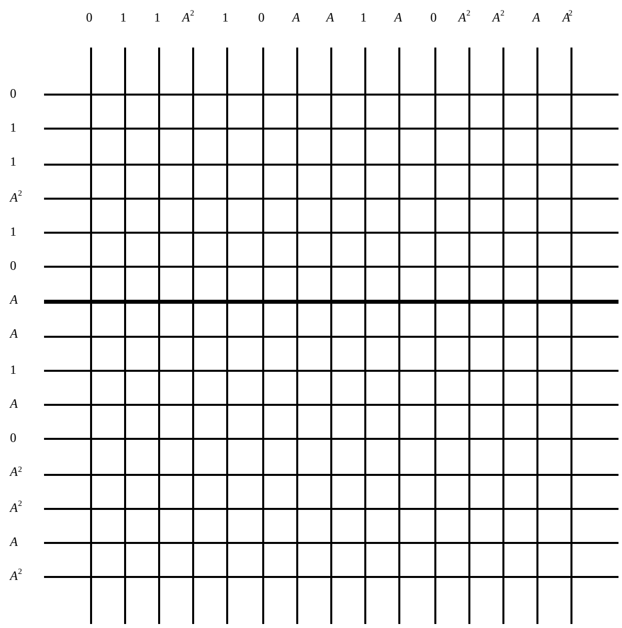


Fig. 3. The 15-by-15 pseudo-random encoded grid.

## 3. Image processing

All the lines of the projected grid have the same thickness as the space between them. Instead of looking for grid-nodes at the intersection of the grid-lines skeletons, we are looking for vertices at the intersection of the grid-line edges. Recovery of the edges will yield the four corner points at the intersection of every two grid lines, while recovering the skeleton of these grid lines will yield only one point. This technique results in a 4:1 increase in the density of the recovered grid points used for triangulation as shown in Fig. 4.

All four corner points found at the intersection of the edges of two grid lines will obviously share the same grid index. To avoid any confusion they are further identified by their relative position: UPPER_LEFT, UPPER_RIGHT, LOWER_LEFT,and LOWER_RIGHT.

Fig. 5 shows an extracted grid with and the recovered lines after edge detection.

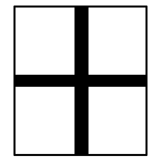

(a) Intersecting grid lines

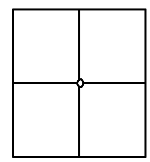

(b) Grid lines after thinning

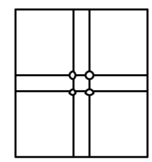

(c) Grid line edges

Fig. 4. Recovering grid nodes at the intersection of grid line skeletons (b) or as corner points at the intersection of grid line edges (c).

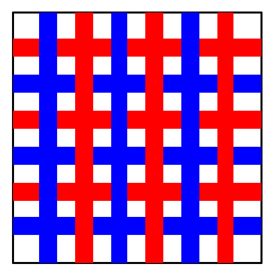

(a) Extracted grid

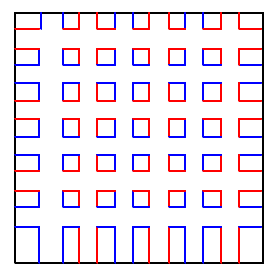

(b) Recovered line edeges

Fig. 5. Image of a grid and its recovered edges

The following considerations have been followed to will reduce errors in the edge recovery process:

(a) connecting only edge points that agree with the pseudo-random color encoding definition;

(b) connecting only edge points that agree with the encoding grid topology.

## 3. Triangulation of the recovered grid points

The 3D geometry of the perspective imaging process is illustrated in Fig. 6. The reference frames of the projector, camera and the world are defined in such a way that their axes *Gx, Gz, Ix, Iz, Wx* and *Wz* are coplanar. $WG = f_1$ is the focal length of the projector's lens, $QI = f_2$ is the focal length of the camera's lens. $WQ = d$ is the fixed distance between the center of the light source and the center of perspective of the camera. *a* is the fixed angle between the focal axis of the projector and *WQ*. *e* is the fixed angle between the focal axis of the camera and *WQ* .

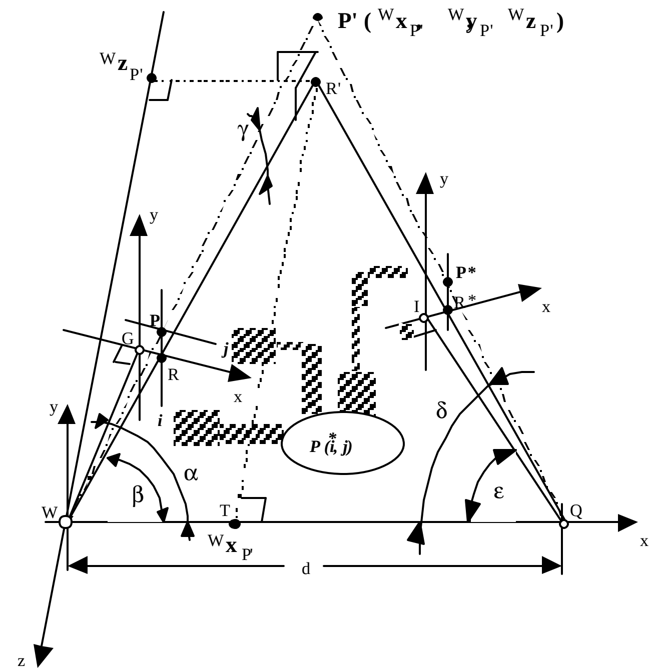


Fig. 6. 3-D perspective geometry for the triangulation of a grid node recovered in the projected image.

After a series calculations we find the 3D coordinates (**x**, **y**, **z**) of the object point *P'* in the world reference system *W*:

$$^{W}\mathbf{x}_{P'} = d \cdot \text{cotg}\, b \ / \ (\text{cotg}\, b + \text{cotg}\, d)$$

$$^{W}\mathbf{y}_{P'} = d \cdot \text{tg}\, g \ / \ [(\text{cotg}\, b + \text{cotg}\, d) \cdot \sin b\ ]$$

$$^{W}\mathbf{z}_{P'} = d \ / \ (\text{cotg}\, b + \text{cotg}\, d)$$

where:

*d* is the fixed distance between the center of the light source and the center of perspective of the camera, and angles *b*, *g*, and *d* are:

$b = a - \text{arctg}\,[(\mathbf{i}\text{-}\mathbf{k})\cdot\Delta x / f_1]$

$g = \text{arctg}\,[(\mathbf{j}\text{-}\mathbf{q})\cdot\Delta y \ / \ \text{sqr}\,(f_1^2 + (\mathbf{i}\text{-}\mathbf{k})^2\cdot\Delta x^2)\ ]$

$d = e + \text{arctg}\,(IR^* / f_2)$

where:

**i** and **j** are the recovered grid coordinates of the pseudo-random encoded grid node *P* which generated the point *P'* on the object's surface;

**k** and **l** are grid coordinates of the point *G* where the focal axis of the projector intersects the encoded grid plane;

*Dx* and *Dy* are the quantization steps along the *x* and *y* axes of the encoded grid plane;

$IR^*$ is a distance measured in the image.

## 3. Experimental results

Experiments were conducted to validate the image processing algorithms and software developed to solve the point identification problem of structured light.

Fig. 7, Fig. 8, and Fig. 9 illustrate the recovery of 3D point parameters on a cube surface using GF(4) pseudo-random encoded structured light.

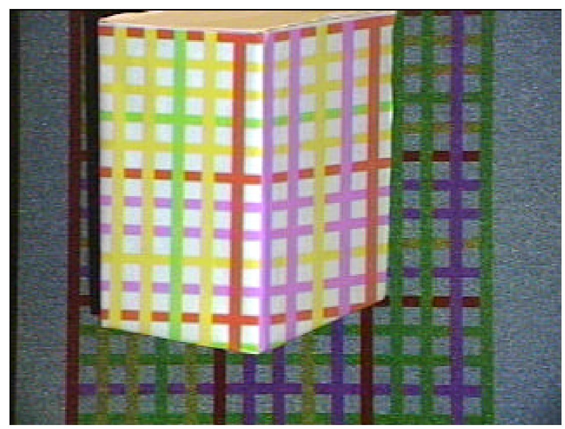

Fig. 7. Image of a pseudo-random color encoded grid projected on a cube

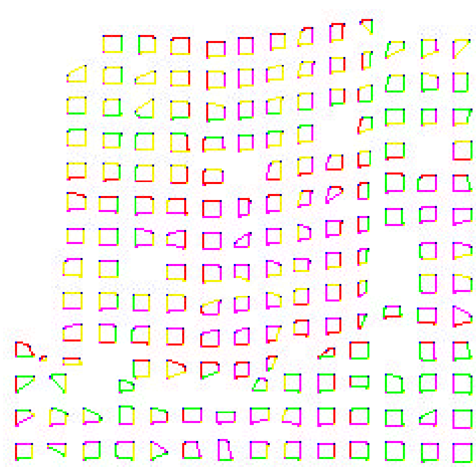

Fig. 8. Recovered corner points at the intersection of grid line edges.

(-1, -1, -1)(84, 18, -1)(-1, -1, -1)(118, 20, -1)(136, 21, -1)
(152, 19, -1)(168, 17, -1)(184, 15, -1)(66, 38, 9.46)
(85, 34, 10.36)(-1, -1, -1)(118, 36, 11.41) (136, 36,11.30)
(152, 35, 11.41)(166, 35, 10.12)(184, 31, 8.49)
(198, 29, 6.63) (-1, -1, -1)(228, 21, 1.48)(244, 20, 1.03)
(66, 50, 9.57) (85, 50, -1)(100, 56, 9.46)(118, 51, 10.36)
(136, 52, 11.81)(152, 52, 11.41)(166, 51, 9.57)
(182, 48, 7.73)(-1, -1, -1)(-1, -1, -1)(228, 38, 1.33)
(244, 37, 1.48)(66, 66, 9.02)(84, 67, 10.36)
(101, 67, 9.95)(118, 67, 10.36)(135, 69, 11.41)
(-1, -1, -1)(166, 67, 9.57)(-1, -1, -1)(-1, -1, -1)(-1, -1, -1)
(226, 55, 0.00)(66, 82, 9.02)(84, 82, 8.44)(101, 83, 9.95)
(118, 83, 9.86)(-1, -1, -1)(-1, -1, -1)(168, 82, 9.38)
(182, 80, 6.57)(180, 146, 7.53) (198, 78, 5.63)
(66, 97, 7.99)(82, 99, 8.10)(100, 99, 9.02)
(117, 100, 9.43)(134, 101, 9.38)(-1, -1, -1)(166, 99, 8.49)
(184, 96, 7.17) (198, 94, 5.18)(-1, -1, -1)(226, 87, 1.33)
(243, 89, 0.66)(66, 115, 8.49) (82, 115, 8.49)(-1, -1, -1)
(116, 118, 10.12)(134, 117, 9.86)(150, 122, 12.46)
(166, 115, 9.02)(182, 113, 7.05)(196, 111, 4.78)
(-1, -1, -1)(-1, -1, 1)(243, 105, 0.94)(65, 131, 7.56)
(-1, -1, -1)(-1, -1, -1)(116, 133, 9.02)(134, 133, 9.86) (150, 133, 9.02)(166, 131, 7.99)(180, 130, 5.93)
(196, 127, -1)(-1, -1, 1)(-1, -1, -1)(243, 123, 0.94)
(64, 147, -1)(82, 147, 7.50) (99, 148, -1)(116, 148, 7.99)
(133, 154, 11.60)(150, 150, 9.02)(166, 147, 7.50)
(-1, -1, -1)(196, 143, 3.75)(-1, -1, -1)(-1, -1, -1)
(243, 138, 1.48)(64, 165, -1)(-1, -1, -1)(99, 165, -1)
(116, 165, 8.49)(133, 168, 10.12)(150, 167, 9.57)
(-1, -1, -1)(-1, -1, -1)(-1, -1, -1)(-1, -1, -1)(-1, -1, -1)
(242, 155, 0.94)(-1, -1, -1)(-1, -1, -1)(-1, -1, -1)
(-1, -1, -1)(-1, -1, -1)(-1, -1, -1)(-1, -1, -1)(-1, -1, -1)
(-1, -1, -1)(-1, -1, -1)(-1, -1, -1)(-1, -1, -1)(-1, -1, -1)
(-1, -1, -1)(-1, -1, -1)(-1, -1, -1)(-1, -1, -1)(-1, -1, -1)
(-1, -1, -1)(175, 188, 1.33)(192, 188, 0.66)(-1, -1, -1)
(226, 188, 0.66)(40, 206, 0.66)(58, 205, 2.10)
(74, 205, 0.66)(92, 204, 1.33)(108, 205, 1.48)
(124, 205, 0.66)(141, 207, 0.94)(158, 205, 1.33)
(176, 205, 0.66)(192, 205, 0.66)(-1, -1, -1)
(226, 206, 0.66)(242, 207, 0.94)

Fig. 9. 3D coordinates of the recovered corner points obtained by triangulation. Negative values indicate recovery errors.

## 5. Conclusion

The described PRMVS encoding provides an unequivocal identification (indexing) method of any grid node projected on an object surface. This encoding requires only two code-symbols per node, independent of the desired resolution. The reconstructed grid appeared sometimes to be incomplete, however the information, which it contains, is still reliable. Extreme perspective distortion can result in incorrect distance measurements.

## Acknowledgment

This work was funded in part by Communications and Information Technology Ontario (CITO) and the Natural Sciences and Engineering Research Council (NSERC) of Canada.

## References

[1] Will P.M., Pennington K.S., "Grid Coding: A Novel Technique for Image Processing," Proc. IEEE, vol. 60, no. 6, pp.669-680, June 1972.

[2] Hall E.L., Tio J.B.K., McPherson C.A., Sadjadi F.A., "Measuring Curved Surfaces for Robot Vision," IEEE Computer, vol. 15, no. 12, pp.42-54, 1982.

[3] Jarvis R.A., "A Perspective on Range Finding Techniques for Computer Vision," IEEE Trans. Pattern Anal. Machine Intell, vol. PAMI-5, no. 2, pp.122-139, 1983.

[4] Arman F., Aggarwal J.K., "Model-Based Object Recognition in Dense-Range Images-A Review," ACM-Computing Surveys, vol. 25, no. 1, pp.5-43, 1993.

[5] Sanderson A.C., Weiss L.E., Nayar S.K., "Structured Highlight Inspection of Specular Surfaces," IEEE Trans. Pattern Anal. Machine Intell, vol. 10, no. 1, pp.44-55, Jan. 1988.

[6] Vuylsteke P., Oosterlink A., "Range Image Acquisition with a Single Binary-Encoded Light Pattern," IEEE Trans. Pattern Anal. Machine Intell, vol. 12, no. 2, pp.148-164, Feb. 1990.

[7] Hu G., Stockman G., "3-D Surface Solution Using Structured Light and Constraint Propagation," IEEE Trans. Pattern Anal. Machine Intell, vol. 11, no. 4, pp.390-402, 1989.

[8] F. J. MacWilliams and N. J. A. Sloane, "Pseudorandom Sequences and Arrays", Proc. IEEE, Vol. 64, No. 12, pp. 1715-1729, Dec. 1976.

[9] E. Petriu, J. S. Basran, "On the Position Measurement of Automated Guided Vehicles Using Pseudorandom Encoding," IEEE Trans. Instrum. Meas., Vol.38, No.3, pp.799-803, 1989.